metals

MDPI

Article

Effect of Preparation Parameter on Microstructure and Grain Refining Behavior of In Situ AlN-TiN-TiB_2/Al Composite Inoculants on Pure Aluminum

Qian Wang, Chunxiang Cui *, Xin Wang, Lichen Zhao, Nuo Li and Shuiqing Liu

Key Laboratory for New Type of Functional Materials in Hebei Province, School of Materials Science and Engineering, Hebei University of Technology, Tianjin 300130, China; wangqian296@163.com (Q.W.); ahaxin@126.com (X.W.); zhlch@hebut.edu.cn (L.Z.); ln0713@126.com (N.L.); liushuiqing0824@126.com (S.L.)

* Correspondence: hutcui@hebut.edu.cn; Tel.: +86-22-2656-4125; Fax: +86-22-6020-4125

Academic Editor: Hugo F. Lopez

Received: 4 January 2017; Accepted: 10 February 2017; Published: 15 February 2017

Abstract: The formation of in situ AlN-TiN-TiB_2/Al composite inoculants, which contain multi-phase refiner particles including AlN, TiN, TiB_2, Al_3Ti, and α-Al, was investigated using nitrogen gas injection. The effects of the main preparation parameters such as nitriding temperature, nitriding time, Ti content in melts, on the microstructure and grain refinement of in situ AlN-TiN-TiB_2/Al composite inoculants were studied. The shape, content and size of different ceramic particles in the inoculants can be tuned by controlling the nitriding temperature and time, inducing excellent refining and reinforcing effects on pure aluminum. As a result, the average grain size of pure aluminum can be reduced to about 122 ± 22 μm from original 1010 ± 80 μm by adding 0.3 wt % inoculants. The mechanical properties including the tensile strength, yield strength and microhardness of the refined as-cast pure aluminum are also improved.

Keywords: in situ Al matrix composite; inoculant; grain refinement; microstructure; aluminum

1. Introduction

Inoculation treatment is a traditional casting technology to refine the microstructure of castings in the field of aluminum alloys. By adding some special master alloys (intermediate alloys) that contain a lot of particles serving as the substrates for heterogeneous nucleation, the grain size of the inoculated alloys can be obviously reduced and the comprehensive properties are improved [1–4]. In fact, most of the master alloys belong to Al-based composites, in which the aluminum-based solid solution is the matrix and the refiner particle is the secondary phase. Here, the secondary phase is generally a ceramic particle, which plays a role of grain refining. For example, in the conventional Al-5Ti-1B inoculants, TiB_2 and Al_3Ti particles provide the substrates for the nucleation of Al crystals. However, the activity of Al_3Ti is strongly affected by the chemical elements contained in an inoculated Al melt. When the Al melt contains special elements, such as Zr, V, and Mn, the performance of Al-5Ti-1B inoculants can sharply deteriorate, namely, with a poisoning effect of Al-5Ti-1B inoculants [5,6]. Moreover, when the concentration of silicon in Al-Si alloys exceeds 3 wt %, the refining effect of Al-5Ti-1B inoculants is greatly reduced due to the formation of Ti_5Si_3 that has a poor crystallographic matching with aluminum matrix [7]. In addition, while improving the amount of TiB_2 particles for more substrates, TiB_2 particles are inclined to agglomerate and precipitate in aluminum melt, which triggers the fading of refinement effect. To change the limitation of Al-5Ti-1B inoculants, other ceramic particles such as CeB_6 [8], LaB_6 [9], TiN [10,11], and B_4C [12], were also introduced to the study of inoculants. In particular, some multi-phase refiners show excellent refining effects on a variety of aluminum alloys, due to the presence of different refiner particles [13]. To sum up, for both single-phase refiners and multi-phase refiners, the amount and distribution of refiner particles play important roles for

the inoculation behavior of composite inoculants [14]. Therefore, the preparation and processing of inoculants alloys, which determines both macro and micro structure of the inoculants, are very important and should be studied.

Recently, in situ AlN-TiN-TiB_2/Al composite inoculants were developed via the gas injection method in our previous work [15]. However, the influence of typical preparation parameters on the grain-refining effect of the inoculants was not described in detail. In this work, five in situ AlN-TiN-TiB_2/Al composite inoculants were prepared via gas injection method to research the influence of the nitriding temperature, nitriding time, Ti content and stirring device on the microstructure and grain refinement of in situ AlN-TiN-TiB_2/Al composite inoculants.

2. Experimental Procedures

Commercial Al-5Ti-1B alloy and titanium sponge with a purity of <99.5% were used as the starting materials. A WK-II-type non-consumable vacuum arc furnace (WuKe Optoelectronics Technology Ltd., Beijing, China) was employed to prepare the as-cast Al-8Ti-1B master alloy. Then, the as-received Al-5Ti-1B alloy and the as-cast Al-8Ti-1B alloy were remelted and treated by nitriding equipment, as shown in Figure 1. The experiment was carried out in a crucible-type resistance furnace (ZhongHuan experimental electric furnace Ltd., Tianjin, China). A highly pure graphite crucible with a graphite lid was used to melt Al-5Ti-1B alloys and Al-8Ti-1B alloys, respectively. The experimental process was as follows: Firstly, the alloy charges of approximately 100 g were heated in the crucible type resistance furnace. When the temperature of the melts reached 1173 K or 1373 K, highly pure nitrogen (purity: 99.997%, O_2 content <6 ppm) was introduced into the melts through the gas-guide tube (Al_2O_3 tube) for 1 h to 2 h at a gas flow rate of 1.0 L/ min. A stirring device was applied to mix the in situ synthetic ceramic particles with the Al melts, homogeneously. The detailed processing parameters for each composite inoculant are listed in Table 1. Finally, the melts after nitridation were then poured into a steel mold, which has a cylindrical cavity with a diameter of 20 mm and a length of 150 mm.

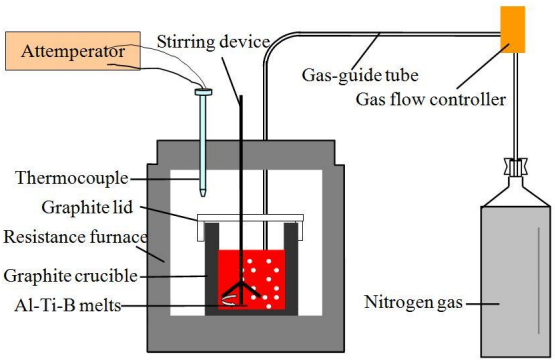

Figure 1. Schematic diagram of the nitrogen injection setup.

Table 1. Processing parameters for the inoculants.

Alloys No.	Composition	Nitridation Temperature (K)	Nitridation Time (h)	Whether the Stirring
A1	Al5Ti1B	1173	1	Stirring
A2	Al5Ti1B	1373	1	Stirring
A3	Al8Ti1B	1373	1	Stirring
A4	Al8Ti1B	1373	2	Stirring
A5	Al5Ti1B	1373	1	Without Stirring

The specimens used for microstructure observation were cut from the surface and center of the ingot, respectively. The specimens were polished using standard metallographic techniques and etched with 0.5 vol % hydrofluoric acid after mechanical polishing. Microstructures and components of specimens were observed and analyzed by Philips XL 30 TMP scanning electron microscopy

(SEM, Royal Dutch Philips Electronics Ltd., Amsterdam, The Netherlands) with energy-dispersive spectrometry (EDS, Royal Dutch Philips Electronics Ltd., Amsterdam, The Netherlands). Philips X'Pert MPD X-ray diffraction (XRD, Royal Dutch Philips Electronics Ltd, Amsterdam, The Netherlands) was used to identify the phase composition of specimens.

The in situ AlN-TiN-TiB_2/Al composites were used as inoculants and added into pure aluminum melts (purity: 99.75%) with an amount of 0.3 wt %. The melts were then stirred with a graphite rod for 30 s. After that, the melts were covered by the flux and hold for 10 min. Then the melts were poured into a steel mold with a size of 100 mm × 100 mm × 150 mm, which had a cylindrical cavity with a diameter of 20 mm and a length of 150 mm. Each metallographic specimen was cut from the middle part of the as-cast rod and polished to remove scratches. The specimens were etched by a reagent (75 mL HCl + 25 mL HNO_3 + 5 mL HF) for macrostructure observation. The grain size analysis was carried out using the linear intercept method. The tensile specimens were machined following standard ASTM E399 and the gauge length was about 50 mm with a diameter of 10 mm. A tensile test was performed on a SHT5305 type microcomputer-controlled electro-hydraulic servo universal testing machine (DunJie Measurement Devices Ltd, Wuhan, China) at a strain rate of ~1×10^{-3} s^{-1}. An HXD-1000 microhardness tester (Shimadzu Corporation, Kyoto, Japan) was used to determine the Vickers microhardness of specimens.

3. Results and Discussion

3.1. Effects of Nitriding Temperature, Nitriding Time, Composition, and Stirring Device on the Formation of In Situ AlN-TiN-TiB_2/Al Composites

The XRD analysis of five in situ AlN-TiN-TiB_2/Al composite inoculants are shown in Figure 2, and Figure 2b is the amplification of Figure 2a from 32° to 39°. It can be seen that sample A1 consists of α-Al, Al_3Ti, and TiB_2 phases, while sample A2, A3, A4, and A5 consist of α-Al, Al_3Ti, TiB_2, AlN, and TiN phases. However, the detailed fraction of Al_3Ti, AlN, and TiN phases in A2, A3, A4, and A5 is significantly different. In Figure 2a A1, there are α-Al, $A1_3Ti$ and TiB_2 peaks in the XRD pattern of the Al-5Ti-1B melt treated at 1173 K for 1 h, whereas TiN and AIN peaks were not found. It is implied that the content of TiN and AIN phases is too little. With the increase of the treatment temperature from 1173 K to 1373 K, the relative intensity of TiN and AIN peaks increases slightly, whereas the $A1_3Ti$ peaks are decreased as shown in Figure 2a A2. As Ti content increases from 5 wt % to 8 wt %, the intensity of $A1_3Ti$, TiN and AIN peaks significantly increases as shown in Figure 2a A3. In addition, as the treatment time is increased from 1 h to 2 h, the relative intensity of TiN and AIN peaks increase as shown in Figure 2a A4. To sum up, the relative intensity of TiN and AlN peaks increase with the increase of nitridating temperature, nitridating time and Ti content in melt.

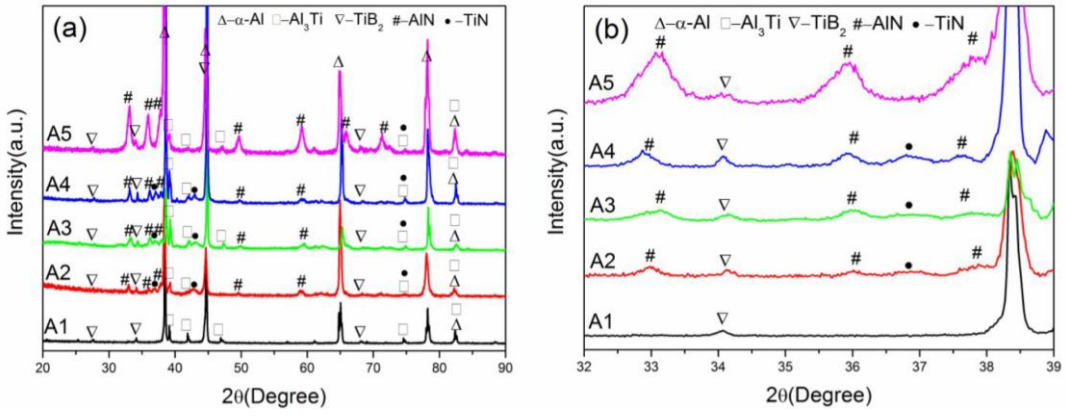

Figure 2. XRD patterns of five in situ AlN-TiN-TiB_2/Al composite inoculants: (**a**) full spectra; and (**b**) partial amplification spectra from 32° to 39°.

If the stirring device is not used, the upper part of the Al-Ti-B melt forms a hard shell during nitridation at 1373 K, while the lower part of the melts remains good fluidity. The hard shell (A5) was peeled off for XRD analysis, as shown in Figure 2 A5. It can be seen that the hard shell consist of massive AlN phase.

The microstructures and EDS analysis of in situ AlN-TiN-TiB_2/Al composite inoculants are shown in Figure 3. From Figure 3a,b, it can be seen that sample A1 is composed of blocky-like Al_3Ti phase and a few TiB_2, AlN and TiN particles. The size of Al_3Ti phases is about ~50 μm and the size of TiB_2, AlN, and TiN particles is about ~1 μm. When the nitriding temperature is increased to 1373 K, the edge of blocky-like Al_3Ti phases occurs bursting crack. Meanwhile, the content of AlN and TiN particles also increases slightly as shown in Figure 3d,e. From Figure 3g,h, it can be seen that A3 composite, which was synthesized by Al-8Ti-1B alloy at 1373 K with the nitriding time of 1 h, is composed of massive blocky-like Al_3Ti phase and massive TiB_2, AlN and TiN particles. The edge of blocky-like Al_3Ti phases crack seriously in A3 composite and the size of Al_3Ti phases decreases. The large increase in the content of blocky-like Al_3Ti phase and TiB_2, AlN and TiN particles are all ascribed to the increase of Ti content in alloy. As it was known, the shape of TiN, AlN, and TiB_2 is square, hexagon and irregular, respectively [13]. Therefore, based on a combining consideration of the XRD results (Figure 2), the morphologies (Figure 3h,k) and the EDS results (Figure 3f,i,l), these particles can be confirmed as AlN, TiN, and TiB_2 phases. When nitriding time increases to 2 h, the size of Al_3Ti phase decrease to ~14 μm and a large number of TiN, AlN and TiB_2 particles are homogeneously formed in the matrix with a size of ~1 μm as shown in Figure 3j,k. Figure 3m,n shows the SEM images of A5, namely, the hard shell in the upper part of the crucible. Combined with the XRD (Figure 2e) and EDS analysis (Figure 3o), it can be seen that the appearance of AlN phase shows a whisker-like shape, very different from the other four. In particular, the AlN whiskers are agglomerated to AlN binds with sizes ranged from nano-scale to micron scale due to the enormous surface energy.

3.2. Thermodynamics Analysis and the Formation Mechanism

The following Reactions (1)–(4) would probably take place in Al-Ti-B melts during the process of nitrogen injection:

$$2Al + N_2 \rightarrow 2AlN \quad (1)$$

$$[Ti] + \frac{1}{2}N_2 \rightarrow TiN \quad (2)$$

$$Al_3Ti \rightarrow 3[Al] + [Ti] \quad (3)$$

$$3[Al] + \frac{3}{2}N_2 \rightarrow 3AlN \quad (4)$$

$$2Ti + N_2 \rightarrow 2TiN \quad (5)$$

where Al and Ti are solid Al and Ti, [Al] and [Ti] are free atoms in the melts (or liquid Al and Ti), N_2 is nitrogen gas, and AlN, TiN, and Al_3Ti are all in solid state.

The temperature dependence of Gibbs free energy changes for Reactions (1),(2),(5) are shown in Figure 4. The lines for Reactions (1) and (5) were directly obtained from the formulas in [16]. From the Gibbs free energy changes, the possibility to form TiN is higher than that of AlN because the Gibbs free energy values of Reaction (5) (TiN) is smaller than Reaction (1) (AlN) as shown in Figure 4. However, the state of Ti in aluminum melt might be none-solid Ti. Thus, there are many titanium atoms ([Ti]) in aluminum melts, which mainly depends on the amount of Ti and the temperature. It is very different from the standard state. The standard Gibbs free energy changes for Ti from puresolid to 1 wt % solute in aluminum melts is [17]:

$$Ti(s) \rightarrow [Ti]\ \Delta G = -97116 - 13.624T \quad (6)$$

When combining Reactions (2) and (6), the Gibbs free energy change of the reaction of [Ti] with N_2, which is as the standard state of 1 wt % Ti in aluminum, can be obtained as shown the line for

R2 in Figure 4. It can be seen that the possibility of the formation of TiN by Reaction (2) is lower than that of AlN by Reaction (1) as shown in Figure 4. This result is in accord with the above experimental result, which is suggested that AlN fraction is much higher than TiN.

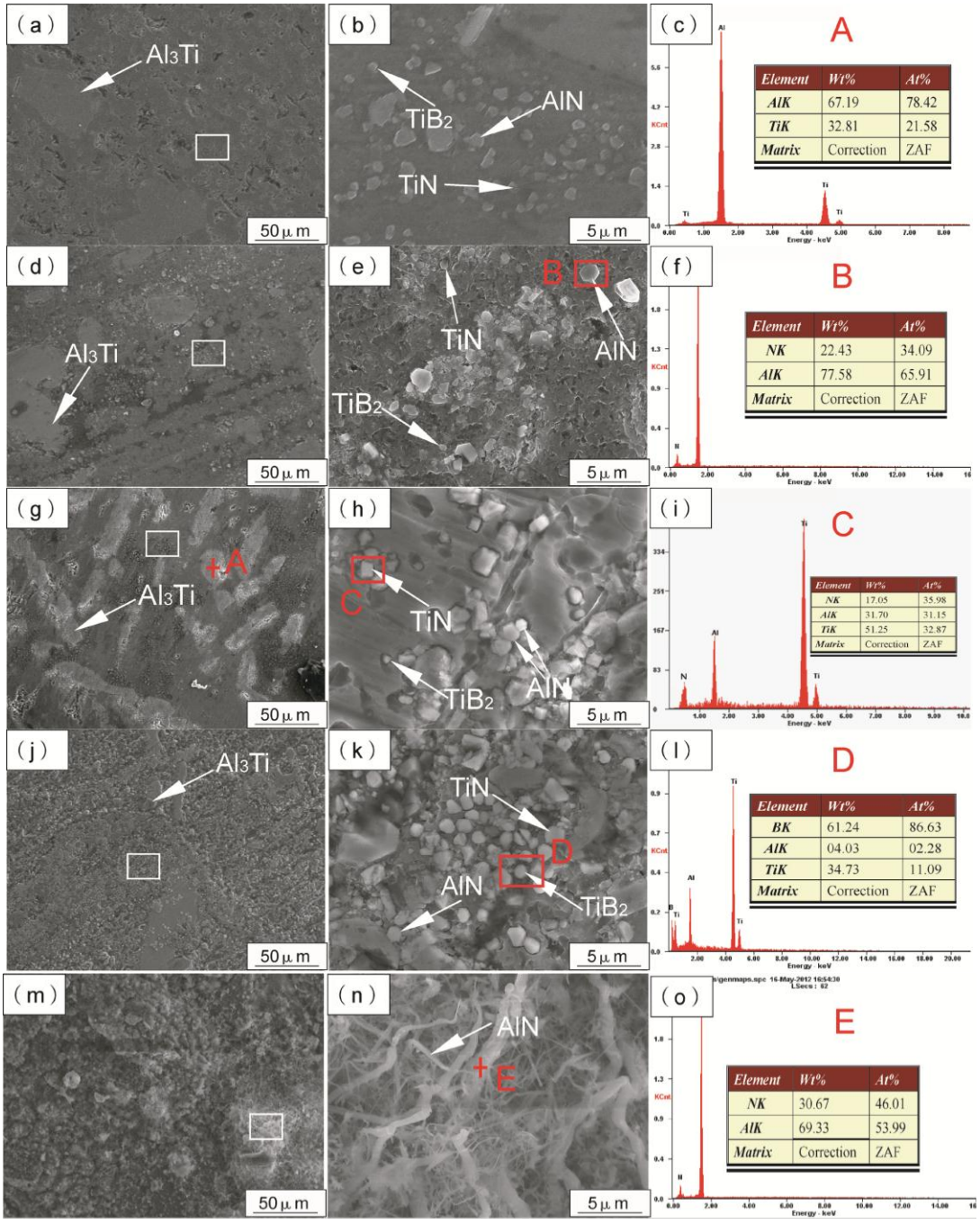

Figure 3. SEM images and EDS analysis of five in situ AlN-TiN-TiB_2/Al composite inoculants: (**a**,**b**) A1; (**d**,**e**) A2; (**g**,**h**) A3; (**j**,**k**) A4; (**m**,**n**) A5; (**c**,**f**,**i**,**l**) and (**o**) are EDS analysis of A, B, C, D, and E points in (**g**,**e**,**h**,**k**,**n**), respectively.

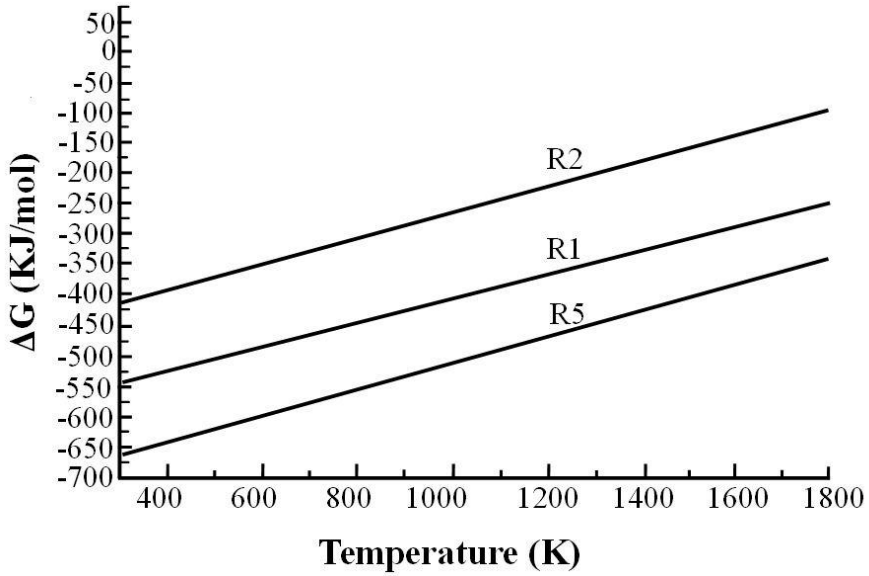

Figure 4. Gibbs free energy changes of the possible reactions for the formation of AlN and TiN as the function of temperature.

According to the binary Ti-Al alloys phase diagram as shown in Figure 5, Al-5Ti-1B melts at 1173 K and Al-8Ti-1B melts at 1373 K are located in the two-phase region (L + $TiAl_3$), so there is equilibrium between phases, which can be expressed as:

$$3[Al]_L + [Ti]_L \rightleftharpoons Al_3Ti_S \quad (7)$$

When [Ti] react with N_2 to form TiN, the concentration of [Ti] in the nitriding Al melt significantly decreases. Then, the reduction of [Ti] would destroy above phase equilibrium (7) and make it develop toward the reverse reaction of (7), leading to the reduction of Al_3Ti phase.

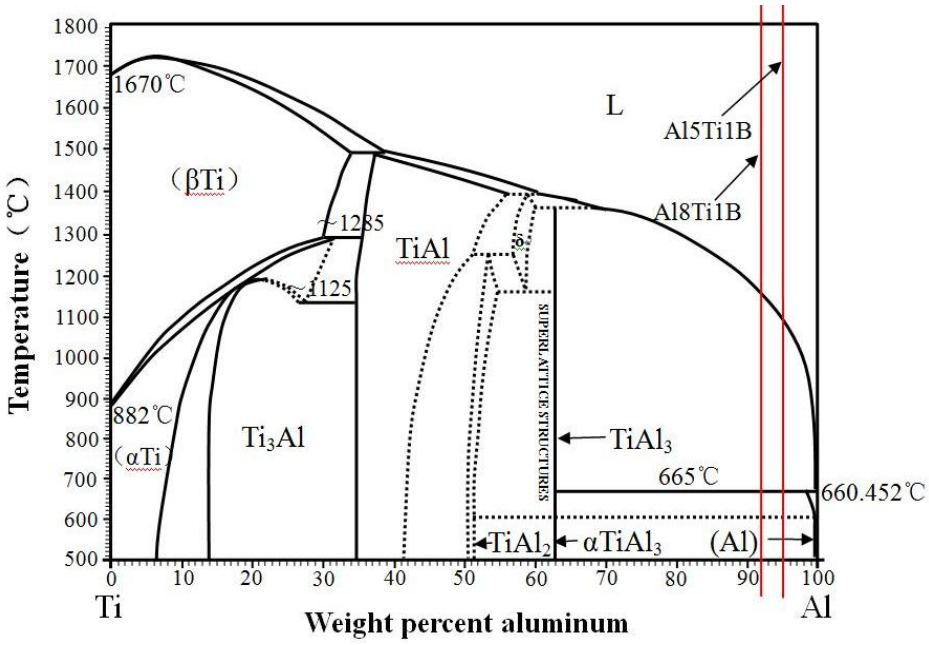

Figure 5. Binary Ti-Al alloys phase diagram.

At high temperature, the amount of solid Al_3Ti is quite small and [Ti] is mainly dissolved in the Al melt. As the melts are cooled, Al_3Ti phase is precipitated from the melt and grows into blocky particle. When N_2 is introduced to the melt with high Ti content, [Ti] is mainly expended by nitridation reaction such that Al_3Ti phase cannot grow into a large strip to make the ceramic particles aggregate.

Based on the above results, Figure 6 shows the schematic of the reactions between N_2 and Al-Ti-B melts. AlN and TiN particles can be directly formed from the reactions during gas injection. The volume fraction of AlN and TiN particles is small during nitrogen injection to Al-5Ti-1B melts at 1173 K for 1 h because of low nitriding temperature, short nitriding time, and low Ti content (as shown in Figure 6a). The volume fraction of AlN and TiN particles dramatically increases during nitrogen injection to Al-8Ti-1B melts at 1373 K for 2 h (as shown in Figure 6b). The volume fraction of AlN and TiN particles increases with the increase of nitriding temperature, nitriding time, and the amount of [Ti] in Al-Ti-B melts. The nitriding reaction mainly takes place at the interface of gas/melt, and the AlN and TiN particles move upwards together with the gas bubbles. The product particles are detached from the interface of gas/melts and enter into the melts due to continuous stirring. When the stirring device is not used, the AlN and TiN particles move upwards together with the gas bubbles and the moving gas bubbles can also absorb TiB_2, AlN, and TiN particles in the melts and move upward together with them. Therefore, the particles can grow up with the continuous deposition of AlN or TiN as shown in Figure 6c.

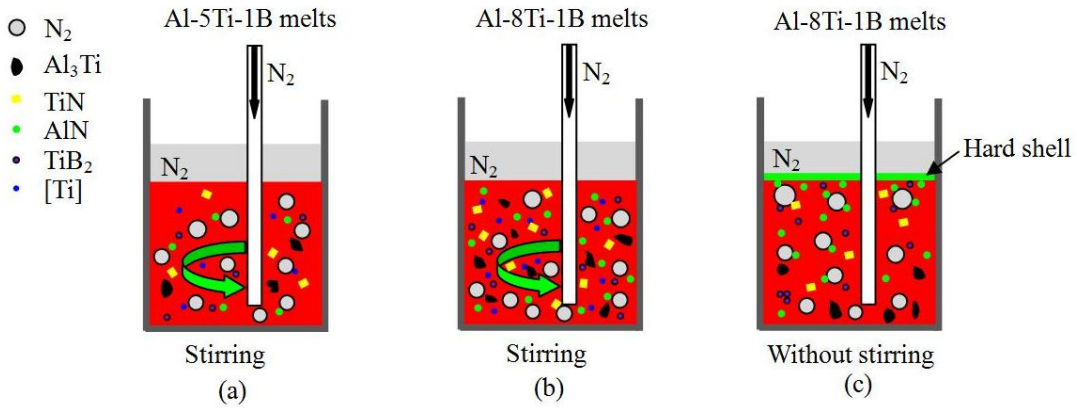

Figure 6. Schematic diagram of different nitriding reactions showing variable conditions: (**a**) A1; (**b**) A4; and (**c**) A5.

3.3. Refining and Reinforcing Effects of the Inoculants on Pure Aluminum

Figure 7 shows the macrostructure of the as-cast pure aluminum sample that is refined by different inoculants with the same addition amount 0.3 wt %. The pure aluminum sample without inoculation exhibits coarse columnar grains. The five in situ AlN-TiN-TiB_2/Al composites all show obvious grain refining effects on pure aluminum, whereas the refining efficiencies are not quite similar. The detailed grain size analysis is shown in Figure 8. The mean grain size of as-cast pure aluminum samples without inoculation is about 1010 ± 80 μm. Based on the quantitative grain size analysis (Figure 8), the grain size of the sample becomes smaller and smaller when the 0.3 wt % A1, 0.3 wt % A2, 0.3 wt % A3, and 0.3 wt % A4 are added into pure aluminum in turn. Interestingly, by adding 0.3 wt % A4, the big grain is obviously refined into small grains with an average of 122 ± 22 μm. It is suggested that the refining effect of in situ AlN-TiN-TiB_2/Al composite inoculants increases with the increase of the volume fraction of AlN and TiN particles. Moreover, such small adding content with significant refining effect suggests A4 as economic inoculants for aluminum alloys.

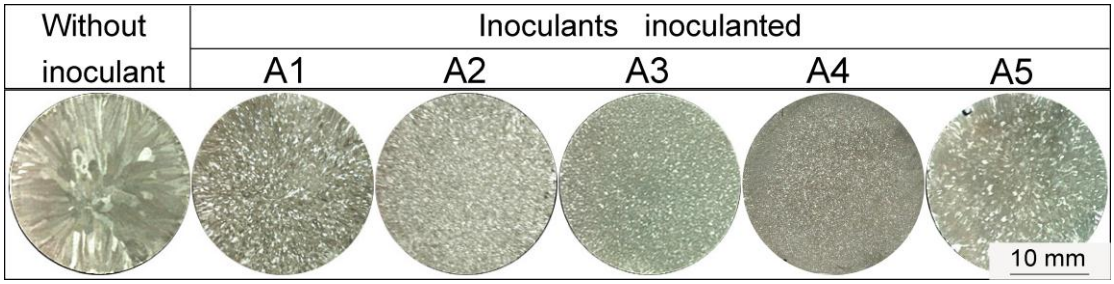

Figure 7. Optical images of Al samples after inoculation with different in situ AlN-TiN-TiB_2/Al composite inoculants.

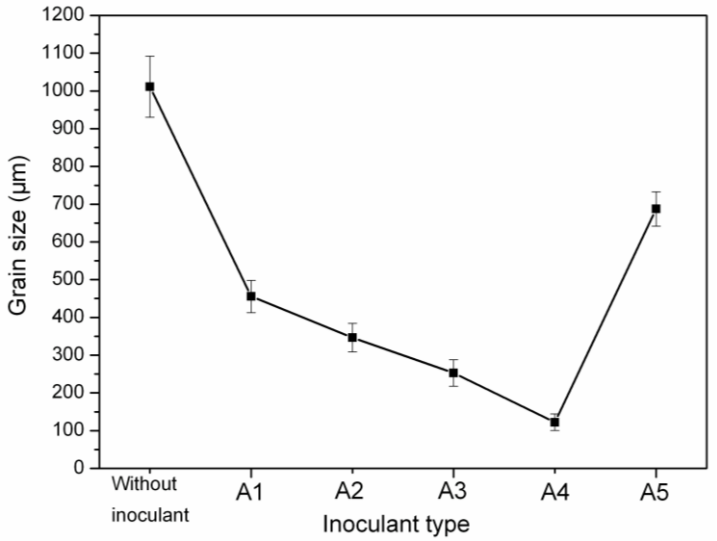

Figure 8. Grain sizes of the as-cast sample inoculated by different inoculants.

The excellent grain refining effect of in situ AlN-TiN-TiB_2/Al composites can be attributed to the following two factors: At the first, Al_3Ti phases become smaller, which provides more substrates for nucleation of α-Al due to the increased specific areas [18,19]. Secondly, a large number of AlN and TiN particles are generated during nitriding besides Al_3Ti phase and TiB_2 particles and these particles dispersed homogeneously in the matrix. This is beneficial for refining aluminum grains. The α-Al phase and TiN phase belong to the face-centered cubic structure. The mismatch degree of the close-packed plane can be expressed by the following equation:

$$\delta = \frac{|d_m - d_p|}{d_p} \tag{8}$$

where d_m is the close-packed spacing of matrix phase, d_p is the close-packed spacing of the precipitate phase. According to the planar lattice mismatch theory presented by Bramfitt [20], the nucleation particles are the most effective with the mismatch of the two phases is less than 6%. The mismatch degree (δ) of several possible coherent interfaces between TiN and Al are shown in Table 2. Based on the calculation results, the mismatch degree between α-Al phase and TiN phase is less than 6%, so it can be used as the most effective nucleating nuclei for the aluminum alloy.

Table 2. Mismatch degree of possible coherent interfaces between TiN and Al.

Number	TiN		Al		δ/%
	d/nm	(hkl)	*d*/nm	(hkl)	
1	0.2440	111	0.2330	111	4.72
2	0.2120	200	0.2020	200	4.95
3	0.1496	220	0.1430	220	4.61
4	0.1227	311	0.1220	311	0.57
5	0.1223	320	0.1170	222	4.53

For AlN phase, the crystal structure is close-packed hexagonal (HCP), different from that of Al.

The lattice constants of Al and AlN are a_{Al} (4.049 × 10^{-10} m) and a_{AlN} (3.113 × 10^{-10} m), c_{AlN} (4.981 × 10^{-10} m), respectively. It can be known that $a_H/a_F = 0.76876$, $c_H/a_H = 1.6$. According to the edge-to-edge matching crystallographic model [21], the match of crystal structures between FCC/HCP systems can be used to calculate the misfit of AlN/Al [22]. In this model, it is reasonable to use 10% and 6% as a critical value for the interatomic spacing misfit and the interplanar spacing misfit. Here, the misfit of $[11\bar{2}0]_H//[110]_F$, $(1\bar{1}01)_H//(1\bar{1}1)_F$ is 1.42% < 6%, 8.73% < 10%, respectively. They both meet the requirements of the critical value. Thus, it is suggested that in situ AlN particles are potential nucleation substrates of aluminum. Furthermore, Cui et al. [23] also found that there existed a crystal parallel relationship between AlN/Al: $(1\bar{1}01)_{AlN}//(1\bar{1}1)_{Al}$. Figure 9 shows the crystal structures of Al, TiN and AlN. Figure 9b is the crystallographic model of Al and AlN. Thus, it is confirmed that $[110]_{Al}$ in $(1\bar{1}1)_{Al}$ can nucleate and grow up along $[11\bar{2}0]_{AlN}$ in $(1\bar{1}01)_{AlN}$.

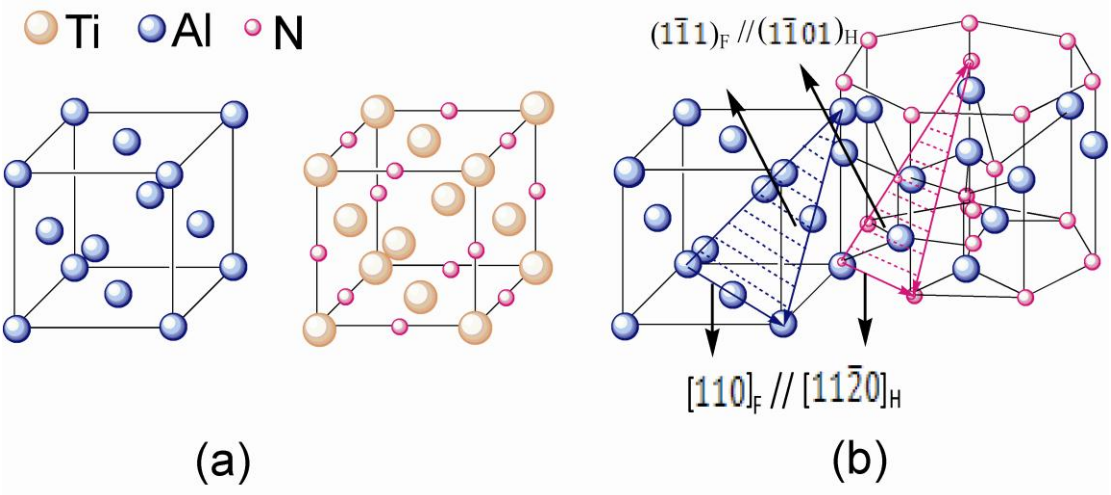

Figure 9. Comparison of crystal cells of (**a**) Al vs. TiN; and (**b**) Al vs. AlN.

Figure 10 shows interface microstructure of in situ formed TiN, AlN, and TiB_2 particles. From Figure 10a it can be found that the ceramic particles have three different size of micron-scale, submicron-scale, and nanometer-scale. Figure 10b shows the interface feature between hexagonal AlN phase and α-Al phase. Figure 10c shows the interface feature between α-Al phase and in situ formed TiN phase, in which a clean interface is observed. Thus, a strong interfacial bonding of the matrix and TiN particles can be obtained. Figure 10d shows the interface feature between α-Al phase and TiB_2 phase. It is found that an Al_3Ti layer is formed on the surface of TiB_2 particles during the grain refiner production process. This phenomena may significantly improve the potency of TiB_2 for nucleation of the α-Al, according to the reported literature [24].

However, the grain size of the sample becomes big when 0.3 wt % A5 is added into pure aluminum. The refining effect of A5 is not obvious because A5 contains a large volume fraction of AlN whiskers in addition to small amounts of Al_3Ti, TiB_2, and TiN, suggesting that AlN whiskers have no effect in the

process of refining. That is because AlN whiskers have a light specific weight, larger specific surface, and strong adsorption, so they are likely to be floating on the surface of the Al melt.

Figure 11 shows the microhardness values of the as-cast Al samples after inoculation with different inoculants. The microhardness values becomes higher and higher with the increased sample number from A1–A4. However, the microhardness values decreases when 0.3 wt % A5 is added into pure aluminum. In particular, the mcirohardness of alloys refined by adding 0.3 wt % A4, has reached up to 107.88 HV, which is improved 162% than that of pure Al without inoculation.

Figure 12 shows the mechanical properties of as-cast pure aluminum samples inoculated with different inoculants. The tensile strength, yield strength, and elongation of pure Al are 41.9 MPa, 28.5 MPa and 37.2%, respectively. The tensile strength and the yield strength of the specimens are both increased, but the elongation is decreased with A1, A2, A3, and A4 inoculant additions. It can be seen that the tensile strength and yield strength increase rapidly up to 109.7 MPa and 77.2 MPa with 0.3 wt % A4 inoculant. Although the elongation of the inoculated materials has a certain decline, the finally value is still in an acceptable level. However, the tensile strength and yield strength decreases as 0.3 wt % A5 is added into pure aluminum. It is suggested that the addition of AlN whiskers do not show an obvious reinforcing effect on pure aluminum. In our opinion, AlN whiskers are light-weight and have larger specific surface and strong adsorption effects, resulting in the whiskers floating on the surface of Al melt. Therefore, AlN whiskers are difficult to be added in the Al melt.

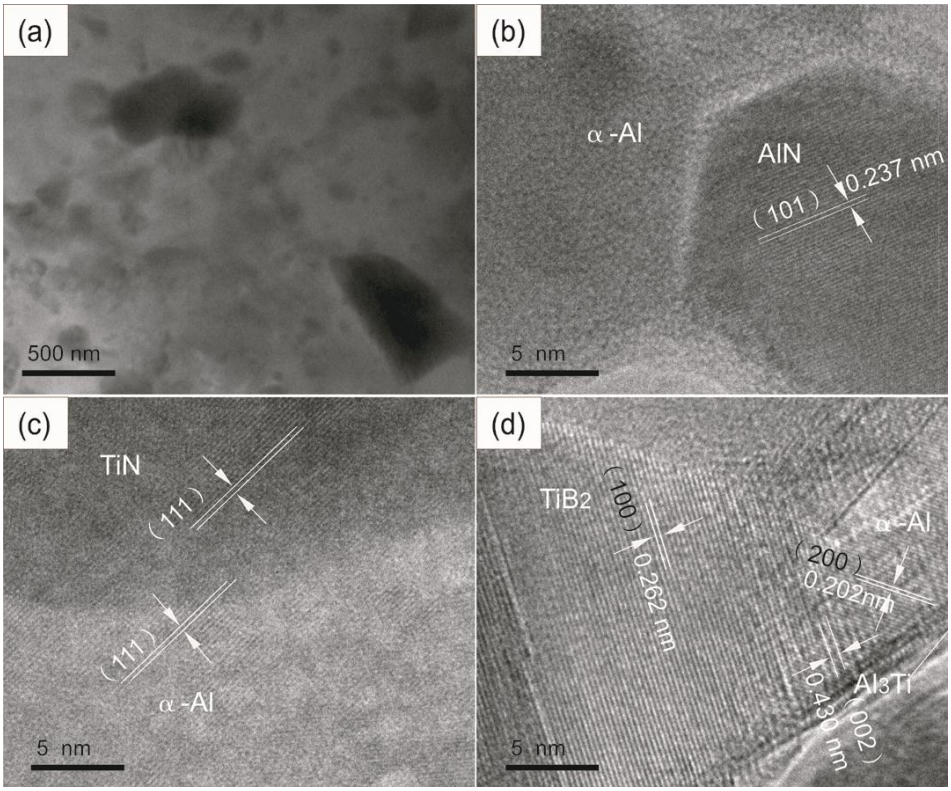

Figure 10. TEM micrographs of in situ formed TiN, AlN, and TiB_2 particles: (**a**) Typical TEM image showing the particles; (**b**) HRTEM image showing a typical Al/AlN interface; (**c**) HRTEM image showing a typical Al/TiN interface; and (**d**) HRTEM image showing a typical Al/TiB_2 interface.

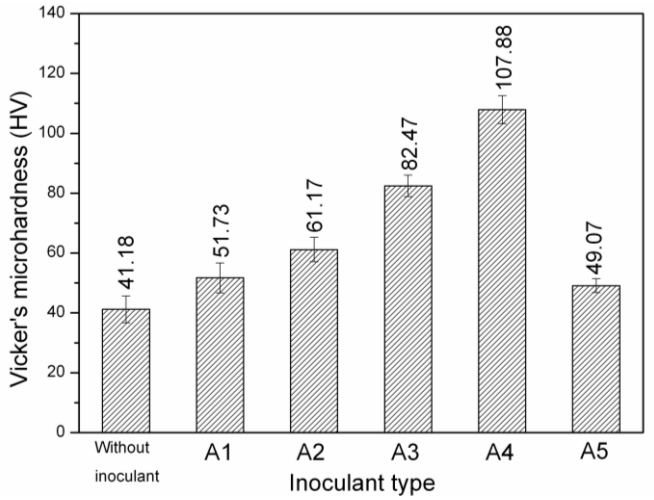

Figure 11. The microhardness of as-cast Al samples after inoculation with different in situ AlN-TiN-TiB_2/Al composite inoculants.

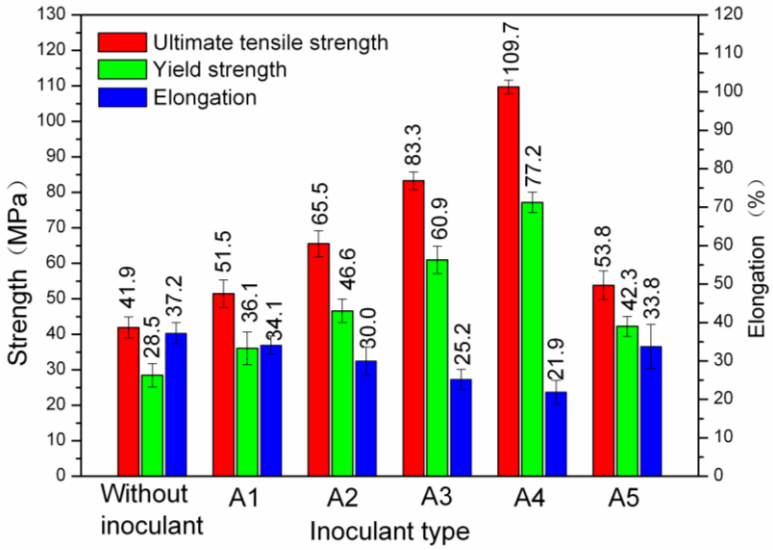

Figure 12. Mechanical properties of the as-cast samples after inoculation with different inoculants.

The improved mechanical properties of pure aluminum modified by in situ AlN-TiN-TiB_2/Al composite inoculants are mainly attributed to the grain refining and particle reinforcing effects. On one hand, according to the Hall-Petch formulation, the yield strength of the composite materials can be expressed as the following equation:

$$\sigma_y = \sigma_i + k_y d^{-\frac{1}{2}} \quad (9)$$

where σ_y is the yield strength, σ_i is a frictional stress resisting the motion of gliding dislocations or an internal back stress, k_y is the Hall-Petch slope which reflects resistance of grain boundary to slip transfer and d is the average grain diameter. From R9, the yield strength of the material is related to the grain size. The smaller the grain size reduced, the higher yield strength can be obtained. In addition, the finer the grain size, the more number of the grain boundaries exist. The grain boundaries can impede dislocation movement and result in the significant improvement of strength of the composite materials, which is called grain boundary strengthening [25]. On the other hand, numerous fine

ceramic particles, such as TiB_2, TiN, and AlN particles, are uniformly distributed in the aluminum matrix and, thus, play an important role of dispersion strengthening. Fine ceramic particles can pin the dislocations and hinder dislocation movement to improve the deformation resistance stress which can ultimately lead to the enhancement of the strength. However, the finer grain size not only makes the material have high hardness and strength [26], but also gives it good plasticity, which means good comprehensive mechanical properties. However, particle reinforcement still leads to a decrease of the elongation of the composites.

4. Conclusions

(1) A multiple phase inoculant, the in situ AlN-TiN-TiB_2/Al composite containing AlN, TiN, TiB_2, Al_3Ti and α-Al, was successfully prepared by nitrogen gas injection. The volume fraction, size, and distribution of TiN and AlN particles can be controlled by tuning the preparation parameters, such as nitriding temperature, nitriding time, Ti content in melt, and stirring.

(2) The refining effect of in situ AlN-TiN-TiB_2/Al composite inoculants increases with the increase of the content of TiB_2, AlN, and TiN particles and the decrease of the size of the Al_3Ti phase. The average grain size of the pure aluminum can be reduced to 122 ± 22 μm from 1010 ± 80 μm by adding of 0.3 wt % A4.

(3) The excellent grain refining effect of in situ AlN-TiN-TiB_2/Al composites is attributed to the miniaturization of Al_3Ti phase, the diversification and homogeneous distribution of ceramic particles, such as AlN, TiN, and TiB_2 particles caused by nitridation and stirring.

(4) The mechanical properties of the pure aluminum have been obviously improved by the addition of in situ AlN-TiN-TiB_2/Al composite inoculants. The tensile strength, yield strength, and microhardness of the pure aluminum are increased from 41.9 MPa, 28.5 MPa, and 41.18 HV to 109.7 MPa, 77.2 MPa, and 107.88 HV.

Acknowledgments: This work is supported by The National Natural Science Foundation of China with No. 51271070, Projects of Natural Science Foundation of Hebei Province with No. E2014202008, Doctoral Foundation of Ministry of Education in China with No. 20131317110002 and The Natural Science Foundation of Tianjin with No. 14JCYBJC17900.

Author Contributions: Qian Wang and Chunxiang Cui conceived and designed the experiments; Qian Wang performed the experiments and wrote the original manuscript; Xin Wang and Chunxiang Cui revised the manuscript and suggested improvements of manuscript; Lichen Zhao, Nuo Li and Shuiqing Liu contributed reagents/materials/analysis tools.

Conflicts of Interest: The authors declare no conflict of interest.

References

1. Zhao, H.L.; Song, Y.; Li, M.; Guan, S.K. Grain refining efficiency and microstructure of Al-Ti-C-RE master alloy. *J. Alloy. Compd.* **2010**, *508*, 206–211. [CrossRef]
2. Wearing, D.; Horsfield, A.P.; Xu, W.W.; Lee, P.D. Which wets TiB_2 inoculant particles: Al or Al_3Ti? *J. Alloy. Compd.* **2016**, *664*, 460–468. [CrossRef]
3. Greer, A.L. Grain refinement of alloys by inoculation of melt. *Phil. Trans. R. Soc. Lond. A* **2003**, *361*, 479–495. [CrossRef]
4. Li, P.T.; Liu, S.D.; Zhang, L.L.; Liu, X.F. Grain refinement of A356 alloy by Al-Ti-B-C master alloy and its effect on mechanical properties. *Mater. Des.* **2013**, *47*, 522–528. [CrossRef]
5. Birol, Y. Grain refining efficiency of Al-Ti-C alloys. *J. Alloy. Compd.* **2006**, *422*, 128–131. [CrossRef]
6. Xu, C.; Xiao, W.L.; Zhao, W.T.; Wang, W.H. Microstructure and formation mechanism of grain-refining particles in Al-Ti-C-RE grain refiners. *J. Rare Earths* **2015**, *33*, 553–560. [CrossRef]
7. Limmaneevichitra, C.; Eidhed, W. Fading mechanism of grain refinement of aluminum-silicon alloy with Al-Ti-B grain refiners. *Mater. Sci. Eng. A* **2003**, *349*, 197–206. [CrossRef]
8. Liu, S.Q.; Wang, X.; Cui, C.X.; Zhao, L.C.; Liu, S.J.; Chen, C. Fabrication, microstructure and refining mechanism of in situ CeB_6/Al inoculant in aluminum. *Mater. Des.* **2015**, *65*, 432–437. [CrossRef]

9. Li, P.T.; Tian, W.J.; Wang, D.; Liu, X.F. Grain refining potency of LaB_6 on aluminum alloy. *J. Rare Earths* **2012**, *30*, 1172–1176. [CrossRef]
10. Li, X.W.; Cai, Q.Z.; Zhao, B.Y.; Li, B.; Liu, B.; Ma, W.L. Grain refining mechanism in pure aluminum with nanosized TiN/Ti composite refiner addition. *J. Alloy. Compd.* **2017**, *699*, 283–290. [CrossRef]
11. Li, X.W.; Cai, Q.Z.; Zhao, B.Y.; Xiao, Y.T.; Li, B. Effect of nano TiN/Ti refiner addition content on the microstructure and properties of as-cast Al-Zn-Mg-Cu alloy. *J. Alloy. Compd.* **2016**, *675*, 201–210. [CrossRef]
12. Shirvanimoghaddam, K.; Khayyam, H.; Abdizadeh, H.; Karbalaei Akbari, M.; Pakseresht, A.H.; Abdi, F.; Abbasi, A.; Naebe, M. Effect of B_4C, TiB_2 and $ZrSiO_4$ ceramic particles on mechanical properties of aluminium matrix composites: Experimental investigation and predictive modeling. *Ceram. Int.* **2016**, *42*, 6206–6220. [CrossRef]
13. Wang, K.; Cui, C.X.; Wang, Q.; Qi, Y.M.; Wang, C. Fabrication of in situ AlN-TiN/Al inoculant and its refining efficiency and reinforcing effect on pure aluminum. *J. Alloy. Compd.* **2013**, *547*, 5–10. [CrossRef]
14. Liu, S.Q.; Wang, X.; Cui, C.X.; Zhao, L.C.; Li, N.; Zhang, Z.; Ding, J.; Sha, D. Enhanced grain refinement of in situ CeB_6/Al composite inoculant on pure aluminum by microstructure control. *J. Alloy. Compd.* **2017**, *701*, 926–934. [CrossRef]
15. Wang, Q.; Wang, X.; Cui, C.X.; Zhao, L.C.; Liu, S.J. Refining and Reinforcing Effects of In-situ AlN-TiN-TiB_2/Al Composite Refiner on Aluminum. *Adv. Eng. Mater.* **2017**, *19*. [CrossRef]
16. Cheng, L.Z.; Han, S.G. *Physical Chemistry*; Shanghai Science and Technology Press: Shanghai, China, 1980; pp. 278–281.
17. Frage, N.; Polak, M.; Dariel, M.P.; Frumin, N.; Levin, L. High-temperature phase equilibria in the Al-rich corner of the Al-Ti-C system. *Metall. Mater. Trans. A* **1998**, *29*, 1341–1345. [CrossRef]
18. Li, P.J.; Kandalova, E.G.; Nikitin, V.I. Grain refining performance of Al-Ti master alloys with different microstructures. *Mater. Lett.* **2005**, *59*, 723–727. [CrossRef]
19. Han, Y.F.; Li, K.; Wang, J.; Shu, D.; Sun, B.D. Influence of high-intensity ultrasound on grain refining performance of Al-5Ti-1B master alloy on aluminium. *Mater. Sci. Eng. A* **2005**, *405*, 306–312. [CrossRef]
20. Bramfittt, B.L. The effect of carbide and nitride additions on the heterogeneous nucleation behavior of liquid iron. *Metall. Trans.* **1970**, *1*, 1987–1995. [CrossRef]
21. Zhang, M.X.; Kelly, P.M. Edge-to-edge matching and its applications: Part I. Application to the simple HCP/BCC system. *Acta Mater.* **2005**, *53*, 1073–1084. [CrossRef]
22. Cao, Y.; Zhong, N.; Wang, X.D.; Huang, B.X.; Rong, Y.H. An edge-to-edge matching model and its application to the HCP/ FCC system. *J. Shanghai Jiaotong Univ.* **2007**, *41*, 586–591.
23. Cui, C.X.; Wu, R.J.; Xue, B.Y.; Li, Y.C. Study of microstructure of AlN/Al interface on in situ TiCp-AlN/Al composite. *J. Chin. Electron Microsc. Soc.* **1998**, *17*, 59–63.
24. Fan, Z.; Wang, Y.; Zhang, Y.; Qin, T.; Zhou, X.R.; Thompson, G.E.; Pennycook, T.; Hashimoto, T. Grain refining mechanism in the Al/Al-Ti-B system. *Acta Mater.* **2015**, *84*, 292–304. [CrossRef]
25. Buban, J.P.; Matsunaga, K.; Chen, J.; Shibata, N.; Ching, W.Y.; Yamamoto, T.; Ikuhara, Y. Grain boundary strengthening in alumina by rare impurities. *Science* **2006**, *311*, 212–215. [CrossRef] [PubMed]
26. Dong, X.X.; He, L.J.; Mi, G.B.; Li, P.J. Two direction microstructure and effects of nanoscale dispersed Si parciles on microhardness and tensile properties of AlSi7Mg melt-spun alloy. *J. Alloy. Compd.* **2015**, *618*, 609–614. [CrossRef]